https://doi.org/10.1093/plphys/kiad603 PLANT PHYSIOLOGY 2023: 00: 1–15

Plant Physiology®

Research Article

Protist ubiquitin ligase effector PbE3-2 targets cysteine protease RD21A to impede plant immunity

Chao Li [1,2,3,4] Shaofeng Luo [1,2] Lu Feng [1,2] Qianqian Wang [1,2] Jiasen Cheng [1,2] Jiatao Xie [1,2] Yang Lin [1,2] Yanping Fu [1,2] Daohong Jiang [1,2] and Tao Chen [1,2,3,4,*]

1 State Key Laboratory of Agricultural Microbiology, Huazhong Agricultural University, Wuhan 430070, China
2 Hubei Key Laboratory of Plant, College of Plant Science and Technology, Huazhong Agricultural University, Wuhan 430070, China
3 Shenzhen Institute of Nutrition and Health, Huazhong Agricultural University, Wuhan 430070, China
4 Shenzhen Branch, Guangdong Laboratory for Lingnan Modern Agriculture, Genome Analysis Laboratory of the Ministry of Agriculture, Agricultural Genomics Institute at Shenzhen, Chinese Academy of Agricultural Sciences, Shenzhen 518120, China

*Author for correspondence: taochen@mail.hzau.edu.cn
The author responsible for distribution of materials integral to the findings presented in this article in accordance with the policy described in the Instructions for Authors (https://academic.oup.com/plphys/pages/General-Instructions) is Tao Chen.

Abstract

Clubroot, caused by the soil-borne protist pathogen *Plasmodiophora brassicae*, is one of the most devastating diseases of *Brassica* oil and vegetable crops worldwide. Understanding the pathogen infection strategy is crucial for the development of disease control. However, because of its obligate biotrophic nature, the molecular mechanism by which this pathogen promotes infection remains largely unknown. *P. brassicae* E3 ubiquitin ligase 2 (PbE3-2) is a Really Interesting New Gene (RING)-type E3 ubiquitin ligase in *P. brassicae* with E3 ligase activity in vitro. Yeast (*Saccharomyces cerevisiae*) invertase assay and apoplast washing fluid extraction showed that PbE3-2 harbors a functional signal peptide. Overexpression of *PbE3-2* in *Arabidopsis* (*Arabidopsis thaliana*) resulted in higher susceptibility to *P. brassicae* and decreases in chitin-triggered reactive oxygen species burst and expression of marker genes in salicylic acid signaling. PbE3-2 interacted with and ubiquitinated host cysteine protease RESPONSIVE TO DEHYDRATION 21A (RD21A) in vitro and in vivo. Mutant plants deficient in *RD21A* exhibited similar susceptibility and compromised immune responses as in *PbE3-2* overexpression plants. We show that PbE3-2, which targets RD21A, is an important virulence factor for *P. brassicae*. Two other secretory RING-type E3 ubiquitin ligases in *P. brassicae* performed the same function as PbE3-2 and ubiquitinated RD21A. This study reveals a substantial virulence functional role of protist E3 ubiquitin ligases and demonstrates a mechanism by which protist E3 ubiquitin ligases degrade host immune-associated cysteine proteases to impede host immunity.

Introduction

Plasmodiophora brassicae, causing clubroot disease worldwide, is an obligate biotrophic pathogen. It produces club-shaped galls by parasitizing the roots of cruciferous plants. The above-ground part of the plant tends to show the symptoms of wilting, stunting, yellowing, premature senescence, or death (Hwang et al. 2012). A global loss of 10% to 15% in yield and 2% to 6% in oil content is attributed to clubroot disease. Clubroot pathogen and disease have been reported in more than 80 countries in the world (Javed et al. 2023). Breeding and cultivation of resistant varieties is the most effective approach to mitigate the threats of this disease (Guo et al. 2022). However, new virulent pathotypes of *P. brassicae* have been constantly emerging (Galindo-González et al. 2020). Understanding the mechanism for successful infection of *P. brassicae* on the host plants will facilitate the breeding of new resistant cultivars and disease management.

P. brassicae is an obligate biotrophic protist appertaining to a subgroup of *Rhizaria*, one of the most poorly understood subsets of eukaryotes. The obligate lifestyle largely hinders investigation of the molecular mechanisms for pathogenic

Received April 18, 2023. Accepted October 18, 2023. Advance access publication November 30, 2023

infection. Delivering effectors into host cells during infection to manipulate plant defenses and facilitate parasitic colonization is an advanced strategy evolved by many eukaryotic biotrophic pathogens (Dodds and Rathjen 2010). Identification of effectors of *P. brassicae* is critical for understanding how the pathogen manipulates the immune response of plants and regulates clubroot resistance. The availability of the genome and transcriptome of *P. brassicae* pathotypes provides an opportunity for identifying the putative effectors (Schwelm et al. 2015; Bi et al. 2016; Rolfe et al. 2016). The first effector identified and characterized in *P. brassicae* is a methyltransferase (PbBSMT), which may methylate salicylic acid (SA) in host cells to manipulate plant immunity (Ludwig-Müller et al. 2015). *P. brassicae* effector SSPbP53 suppresses plant immunity by inhibiting cruciferous papain-like cysteine proteases (PLCPs) (Pérez-López et al. 2021). *P. brassicae* RxLR effector that contains zinc finger Myeloid-Nervy-DEAF1 (PBZF1) interacts with and inhibits the biological function of SnRK1.1. Heterologous expression of *PBZF1* in *Arabidopsis* (*Arabidopsis thaliana*) increases the susceptibility of plants to *P. brassicae* (Chen et al. 2021). To better understand the pathogenic mechanism of *P. brassicae*, it is necessary to further study the roles and molecular mechanisms of *P. brassicae* effector candidates.

Ubiquitination, an important posttranslational modification of proteins unique to eukaryotes (Hershko and Ciechanover 1998), serves as a degradation signal or changes the property of the target protein (Smalle and Vierstra 2004). Usually, ubiquitin ligase E3 can specifically recognize target proteins and is therefore particularly important and extensively studied. Ubiquitination is involved in various mechanisms including cell cycle, apoptosis, protein degradation, and immune regulation and is therefore one of the most important mechanisms regulating various life activities (Hershko and Ciechanover 1998; Smalle and Vierstra 2004; Kim et al. 2010). To date, 139 putative E3 ubiquitin ligases have been predicted in the *P. brassicae* e3 genome, among which PbRING1 contains a functional signal peptide and has E3 ligase activity in vitro (Yu et al 2019). However, the biological functions of E3 ubiquitin ligases in *P. brassicae* remain largely unknown.

Many studies have revealed that ubiquitination is extensively involved in the regulation of plant immunity (Zhou and Zeng 2017). *A. thaliana* E3 ubiquitin ligases PUB12/PUB13 and PUB22 ubiquitinate the pattern recognition receptor FLS2 and the exocyst complex subunit Exo70B2, respectively, to promote their degradation to attenuate PAMP-triggered immune (PTI) signaling (Lu et al. 2011; Stegmann et al. 2012). Besides, PUB12/PUB13 also mediates the degradation of abscisic acid (ABA) coreceptor ABI1 to regulate ABA signaling (Kong et al. 2015). In addition, pathogens secrete effectors to influence plant immunity by regulating the host ubiquitination system. Rice (*Oryza sativa*) E3 ligases APIP6 and APIP10 are targeted by *Magnaporthe oryzae* effector AvrPiz-t, resulting in weakened PTI (Park et al. 2012, 2016). AvrptoB, a type III effector with E3 ligase activity, is important for the pathogenicity of *Pseudomonas syringae* (Abramovitch et al. 2006).

This study aims to investigate the biological functions of secreted E3 ubiquitin ligases in *P. brassicae* and understand the mechanisms for ubiquitination in clubroot development. Our findings indicate that the protist pathogen E3 ubiquitin ligases ubiquitinate the plant cysteine protease RD21, thereby suppressing plant immunity for successful infection.

Results

PbE3-2 is a RING-type E3 ubiquitin ligase

By using Blast2GO to systemically investigate the genome of *P. brassicae* ZJ-1 (Bi et al. 2019), 60 genes were predicted to encode putative E3 ubiquitin ligases (Supplemental Table S1). We hypothesized that some of these E3 ubiquitin ligases are secreted into the host cell and contribute to successful infection. Five out of the 60 predicted E3 ubiquitin ligases possessed signal peptides, which were designated as PbE3-1, PbE3-2, PbE3-3, PbE3-4, and PbE3-5, respectively (Supplemental Table S1 and Fig. S1A). PbE3-1 and PbE3-5 were predicted to have transmembrane domain, while the remaining 3 PbE3s had no such domain (Supplemental Fig. S1A). Reverse transcription quantitative PCR (RT-qPCR) analysis indicated that these 5 PbE3s have differential expression patterns at different life stages of *P. brassicae*, and PbE3-2, PbE3-3, and PbE3-4 were highly expressed during cortex infection (secondary infection) (Supplemental Fig. S1B). PbE3-2 harbored a Really Interesting New Gene (RING) finger domain (Supplemental Table S1) and is conserved among *P. brassicae* pathotypes (Supplemental Fig. S1C). The RING finger domain of PbE3-2 contained 8 conserved Cys/His amino acid residues and thus belonged to the $C_3H_2C_3$-type family (Fang and Weissman 2004) and could coordinate 2 Zn^{2+} ions (Fig. 1A). The 3D model of the RING finger domain in PbE3-2 was similar to that of the canonical RING from maize (*Zea mays*) (Fig. 1B). We first tested whether PbE3-2 has an enzymatic activity for self-ubiquitination. AtUBA1-S (E1 activating enzyme), AtUBC8-S (E2 conjugating enzyme), PbE3-2-Myc, and His-FLAG-UBQ10 (ubiquitin) were expressed in *Escherichia coli* DE3 strains, and self-ubiquitination of PbE3-2 was tested in the presence or absence of E1, E2, and ubiquitin. PbE3-2 was converted into a mixture of high-M_r ubiquitinated protein products (Fig. 1C), indicating the ability of PbE3-2 to self-ubiquitinate. The PbE3-2 (C423S) mutant was generated by replacing the cysteine residue in the RING structure at Position 423 with a serine. As a result, PbE3-2 (C423S) showed no self-ubiquitination (Fig. 1C). Therefore, PbE3-2 is an E3 ubiquitin ligase.

PbE3-2 suppresses BAX-induced cell death

Secretory proteins, as candidate effectors, are important for the interaction between *P. brassicae* and its hosts (Pérez-López et al. 2018). To determine whether PbE3-2 is secretory, we constructed 2 plasmids expressing PbE3-2-GFP

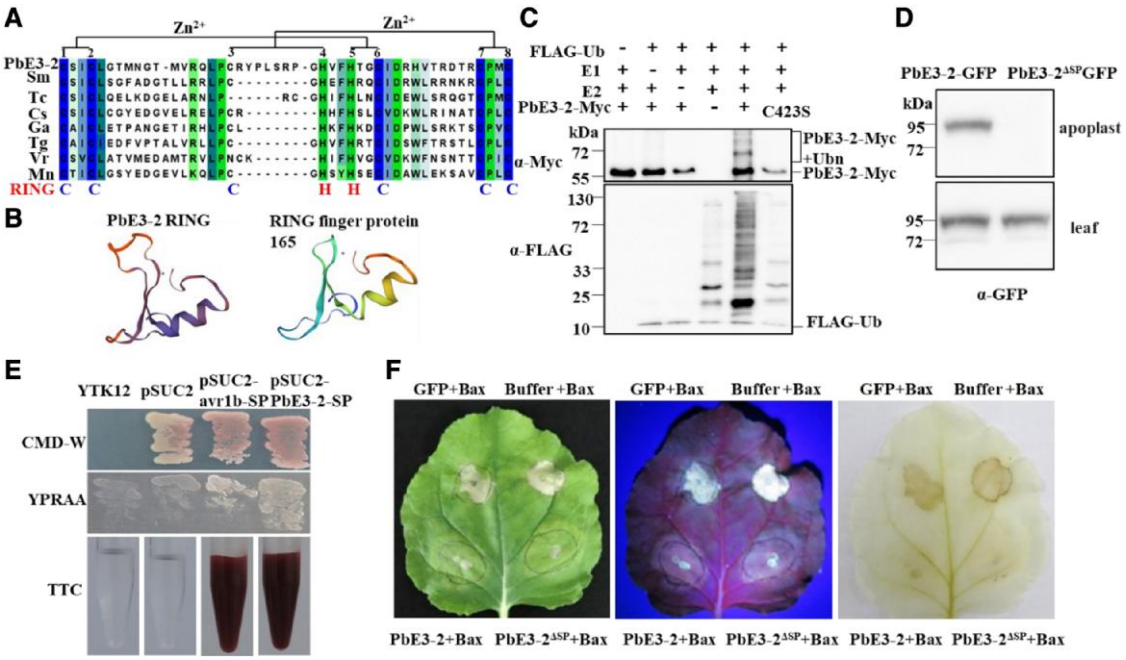

Figure 1. PbE3-2 is a secreted E3 ubiquitin ligase and suppressed BAX-induced cell death. **A)** Protein alignment of PbE3-2 RING and its homologs (*Symbiodinium microadriaticum* OLP82957.1, *Theobroma cacao* EOY12354.1, *Camelina sativa* XP_010413448.1, *Gossypium arboretum* KHG04456.1, *Toxoplasma gondii VEG* CEL71473.1, *Vigna radiata* var. *radiata* XP_014517466.1, and *Monoraphidium neglectum* XP_013905359.1). **B)** Structures of PbE3-2 RING and RING finger protein 165 (*Z. mays*). **C)** Self-ubiquitination of PbE3-2. Ub, E1, E2, and PbE3-2 are all present in the reconstituted systems. PbE3-2 can undergo self-ubiquitination. The system lack of any component is a negative control. The PbE3-2 (C423S) mutant is also unable to undergo autoubiquitination. **D)** PbE3-2-GFP and PbE3-2$^{\Delta SP}$GFP infiltrated to *N. benthamiana* leaves for 2 d, apoplast washing fluid was extracted, and western blotting with GFP antibody indicated that PbE3-2-GFP but not PbE3-2$^{\Delta SP}$GFP was detected in the apoplast washing fluid. **E)** The signal peptide of PbE3-2 has a secretory function. Clones carrying the pSUC2 plasmid can be grown in CMD-W medium (0.67% yeast N base without amino acids, Trp dropout supplement, 2% [w/v] sucrose, 0.1% [w/v] glucose, and 2% [w/v] agar). Yeast secreted invertase degrades cottonseed on YPRAA medium (1% [w/v] yeast extract, 2% [w/v] peptone, 2% [w/v] raffinose, 2-μg/L antimycin A, and 2% [w/v] agar) for growth. TTC is reduced by invertase to red insoluble formazan. pSUC2-avr1b is used as a positive control and pSUC2 empty vector as a negative control. **F)** PbE3-2 and PbE3-2$^{\Delta SP}$ suppressed BAX-induced cell death. PbE3-2 and BAX coinfiltrated to *N. benthamiana* leaves, and BAX and PVX-GFP coinfiltrated as a negative control. Left picture was taken at 5 d after infiltration under visible light, middle picture was taken under UV light, and right picture was decolorization with 75% (v/v) acetic acid and 25% (v/v) alcohol buffer. Experiments were independently performed 3 times with similar results.

fusion proteins with (PbE3-2-GFP) and without signal peptide (PbE3-2$^{\Delta SP}$-GFP) and delivered them into *Nicotiana benthamiana* epidermal cells via *Agrobacterium tumefaciens*. Apoplast washing fluid was extracted, and western blotting indicated that PbE3-2 but not PbE3-2$^{\Delta SP}$ was detected in the apoplast washing fluid (Fig. 1D), suggesting that PbE3-2 is most likely a secretory protein. The secretory nature of PbE3-2 was also confirmed by yeast invertase assay (Fig. 1E). Transient expression assays in the *N. benthamiana* model system have been performed to identify effectors in bacteria, oomycetes, fungi, nematodes, and protist *P. brassicae* (Zhan et al. 2022). Many predicted candidate effectors of *P. brassicae* were assessed by inducing cell death or suppressing plant immunity triggered by BAX in *N. benthamiana* (Chen et al. 2019; Zhan et al. 2022). Thus, PVX plasmid constructs of PbE3-2 or GFP were coexpressed with Bax in *N. benthamiana* leaves (Fig. 1F). PbE3-2 and PbE3-2$^{\Delta SP}$ but not GFP suppressed BAX-induced cell death in infiltrated leaves. These results indicated that PbE3-2 is a candidate effector that suppresses BAX-induced cell death.

PbE3-2 promotes the development of clubroot

To characterize the biological functions of PbE3-2, we generated stable transgenic *A. thaliana* lines constitutively expressing the PbE3-2 coding sequence. Independent homozygous *A. thaliana* lines (OX2, OX5, and OX6) were identified by using western blotting analysis (Supplemental Fig. S2, A and B). The transgenic plants displayed similar growth phenotypes to Col-0 plants (Supplemental Fig. S2A). To determine whether PbE3-2 contributes to clubroot disease, transgenic lines and Col-0 were challenged with *P. brassicae*, and the phenotype was investigated at 21 d postinoculation (dpi) (Fig. 2A; Supplemental Fig. S2C). The roots of wild-type plants showed the formation of typical galls and correspondingly fewer rootlets, and severe galls (disease classes 5) accounted for 12.8% of the total (Fig. 2, A and B); besides, the infected plants exhibited purple leaves (Supplemental Fig. S2C). The PbE3-2 transgenic lines showed more severe symptoms than Col-0, with severe galls (disease classes 5) on the roots accounting for 50% to 60%, and leaves were dark purple and yellow (Fig. 2, A and B; Supplemental Fig.

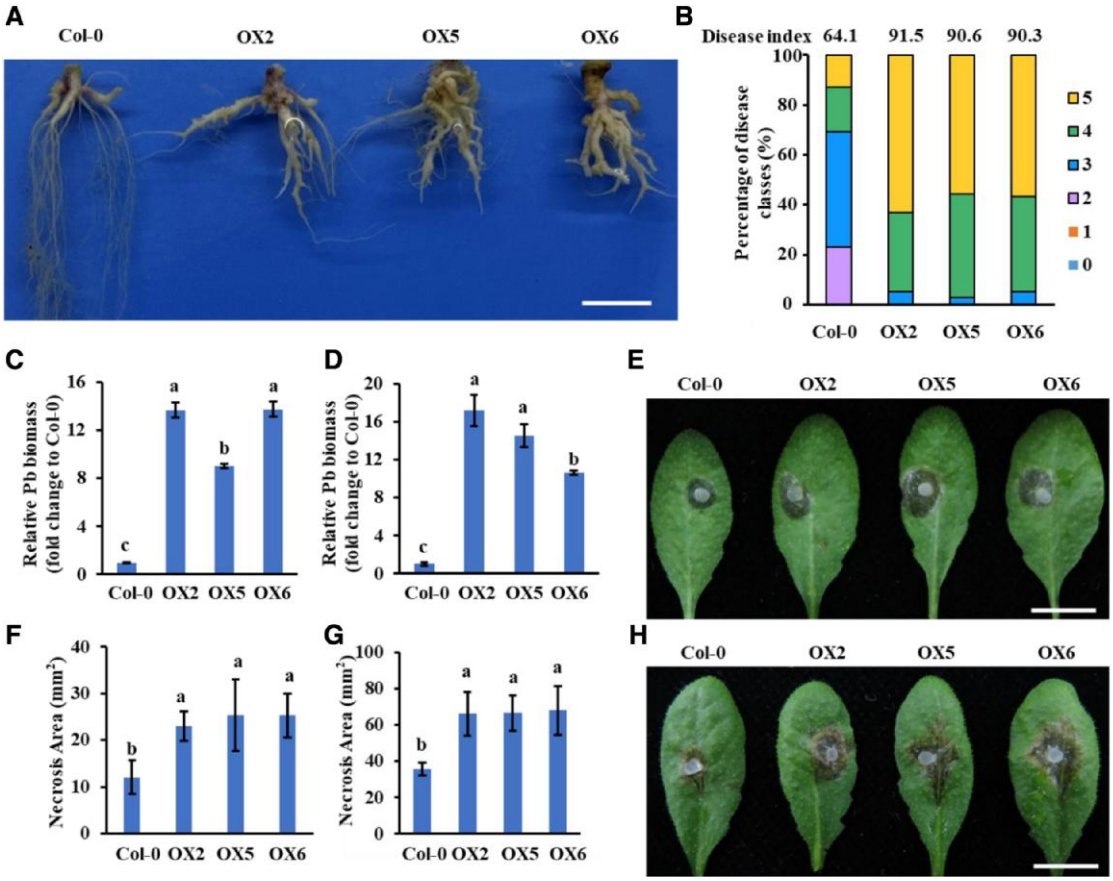

Figure 2. *PbE3-2* overexpression plants are more susceptible to pathogens. **A, B)** Col-0 and *PbE3-2* overexpression plants inoculated with *P. brassicae* for 21 d. Root phenotype of Col-0 and *PbE3-2* overexpression plants inoculated with *P. brassicae* **A)**. Bar: 1 cm. Disease index of Col-0 and *PbE3-2* overexpression plants inoculated with *P. brassicae* **B)**. Percentages of plants in the individual disease classes are shown. For transgenic lines and Col-0 plants, 35 to 40 plants were analyzed. The disease index for each sample is shown as a number above the respective histograms. The experiment was conducted with 3 independent replications with similar results. **C, D)** Quantification of *P. brassicae* content in diseased roots of *Arabidopsis* by qPCR, and the vertical coordinates indicate the multiplicity of Pb content in different lines relative to Col-0. The relative biomass of *P. brassicae* is represented by the content of the *P. brassicae ACTIN* gene relative to that of the *Arabidopsis ACTIN2* gene **C)** and the content of the *P. brassicae DC1* gene relative to that of the *Arabidopsis GAPDH* gene **D)**. Relative Pb biomass is presented as the means ± SD $n = 3$ biological replicates. Bar: 1 cm. Experiments were repeated 3 times with similar results. **E, F)** Col-0 and *PbE3-2* overexpression plants were inoculated with *B. cinerea*; pictures were taken at 24 h postinoculation (hpi) **E)**, and disease spot area data **F)** are presented as the means ± SD ($n = 10$ biological replicates). Bar: 1 cm. Experiments were repeated twice with similar results. **G, H)** Col-0 and *PbE3-2* overexpression plants were challenged with *S. sclerotiorum*, 30 hpi **H)** and disease spot area after inoculation of *S. sclerotiorum* in Col-0 and *PbE3-2* overexpression plants **G)**. Data are presented as the means ± SD ($n = 10$ biological replicates). Bar: 1 cm. Experiments were repeated twice with similar results. Statistical tests used in **C), D), F),** and **G)** were 1-way ANOVA with Kruskal–Wallis test (significance set at $P \leq 0.05$). Different letters (a, b, and c) indicate significant differences.

S2C). The disease index of Col-0 was 64.1, while that of transgenic lines was 90.3 to 91.6 (Fig. 2B). Quantification of *P. brassicae* biomass showed that *PbE3-2* transgenic plants had a more than 10-fold higher amount of *P. brassicae* than Col-0 (Fig. 2, C and D). These results indicated that PbE3-2 transgenic plants are more susceptible to *P. brassicae* than Col-0. Although *P. brassica* is a biotrophic pathogen, its effector PbE3-2 may interfere with the overall immune level of the plant, thereby affecting the resistance to necrotrophic pathogens. Hence, we assessed the susceptibility of *PbE3-2* transgenic lines to the necrotrophic fungi *Botrytis cinerea* and *Sclerotinia sclerotiorum*. As a result, the *PbE3-2* transgenic lines exhibited more significant symptoms of fungal infection than Col-0 (Fig. 2, E to H), indicating that PbE3-2 also modulates the susceptibility of *A. thaliana* to necrotrophic pathogens.

PbE3-2 suppresses plant immune response

To complete its life cycle, *P. brassicae* needs to evade from or downregulate PAMP-triggered immunity (Pérez-López et al. 2021). PTI plays a prominent role in curtailing pathogen invasion (Melotto et al. 2006) and leads to a number of overlapping downstream outputs, such as MAP kinase (MAPK) cascades, calcium flux, reactive oxygen species (ROS) burst, and transcriptional reprogramming (Devendrakumar et al. 2018; Peng et al. 2018). We tested whether PbE3-2 suppresses

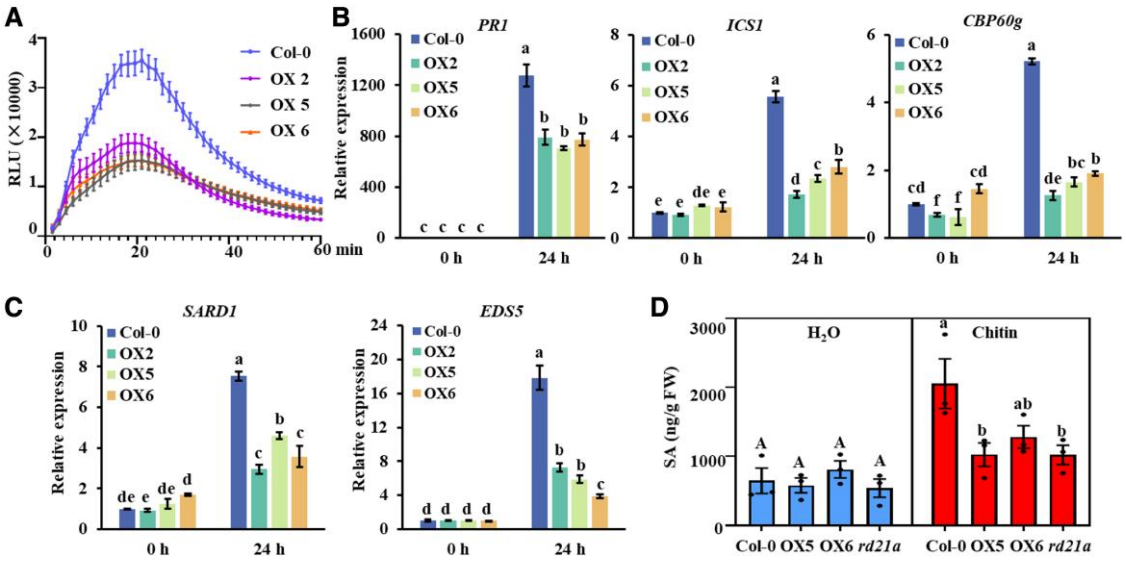

Figure 3. PbE3-2 suppresses plant immune response. **A)** Chitin-induced ROS burst is suppressed in *PbE3-2* overexpression lines. The values represent means ± SE ($n = 16$ biological replicates). Experiments were repeated 3 times with similar results. **B, C)** Induction of the salicylate pathway genes was compromised in *PbE3-2* overexpression lines. Leaves of 4-wk-old plants were infiltrated with 20-μg/mL chitin for 24 h. Data were normalized to *ACTIN2* expression in qPCR analysis. Statistical analysis in **B)** and **C)** were performed by 1-way ANOVA with Kruskal–Wallis test (significance set at $P \leq 0.05$). Different letters (a, b, c, d, and e) are significantly different. $n = 3$ biological replicates; data are shown as mean ± SD. Experiments were repeated 3 times with similar results. **D)** Salicylic acid metabolite quantification of 24 h after hand infiltration with 20 μg/mL of chitin or H_2O of 4-wk-old *Arabidopsis* leaves. Statistical analysis was performed by 1-way ANOVA with Kruskal–Wallis test (significance set at $P \leq 0.05$). Different letters (a and b) indicate significant differences. $n = 3$ biological replicates; data are shown as mean ± SE.

typical immune responses such as ROS burst, MAPK activation, and immune gene induction in response to PAMP. Chitin-triggered ROS burst was reduced by about 50% in *PbE3-2* transgenic plants relative to Col-0 (Fig. 3A). Moreover, the induced expression of *RBOHD* was also remarkably suppressed in PbE3-2 transgenic plants (Supplemental Fig. S3A). However, a comparative analysis of MAPK activation showed no substantial difference between these treatments (Supplemental Fig. S3B). The SA signaling pathway is a central pathway for plant defense against *P. brassicae* (Vlot et al. 2009; Ludwig-Müller et al. 2015; Chen et al. 2016). We compared the induction levels of marker genes of the SA signaling pathway to chitin treatment in PbE3-2 transgenic lines and Col-0 plants. As expected, the induced expression of these marker genes was suppressed in the *PbE3-2* transgenic lines (Fig. 3, B and C). Under the induction of chitin, SA accumulation in *PbE3-2* transgenic lines was significantly decreased compared with Col-0 (Fig. 3D). These results indicated that PbE3-2 may suppress PTI responses by manipulating host ROS burst or SA signaling pathway consistently with our observation that PbE3-2 promotes clubroot disease.

PbE3-2 interacts with the plant cysteine protease RD21A

To identify the host target of PbE3-2, *35S:PbE3-2-GFP* transgenic *A. thaliana* lines infected with *P. brassicae* were prepared. Immunoprecipitation (IP) and liquid chromatography–MS (LC-MS) identified 268 potential interacting proteins of PbE3-2 (Supplemental Table S2). We next screened *A. thaliana* cysteine protease RESPONSIVE TO DEHYDRATION 21A (RD21A) in the yeast 2-hybrid (Y2H) system and in yeast PbE3-2 interacted with RD21A (Fig. 4A). The interaction was validated with a split-luciferase (LUC) complementation assay (Fig. 4B; Supplemental Fig. S5C) and further examined by Co-IP assay by tagging PbE3-2 with GFP whereas tagging RD21A with FLAG, which were coexpressed in *N. benthamiana* leaves. As shown in Fig. 4C, FLAG-tagged RD21A could be coimmunoprecipitated with GFP-tagged PbE3-2. These results indicated that PbE3-2 interacts with RD21A in planta. We further verified the interaction between PbE3-2 and RD21A using a pull-down assay in vitro. PbE3-2 was fused with His tag and RD21A was fused with glutathione S-transferase (GST), which were purified, incubated, and then immobilized to glutathione sepharose beads. Immunoblotting with α-His antibody detected that PbE3-2 was pulled down by RD21A-GST but not GST (Fig. 4D). We coexpressed PbE3-2 and RD21A in plant cells as recombinant proteins fused with split yellow fluorescent protein tags. Poor fluorescent signals were detected in the plasma membrane and cytoplasm (Supplemental Fig. S4A). Interestingly, when PbE3-2 (C423S) and RD21A were coexpressed in plant cells with split red fluorescent protein tags, strong red fluorescent signals were observed in the plasma membrane and the cytoplasm of leaf cells (Fig. 4E), suggesting that PbE3-2 (C423S) and RD21A interact with each other in plant cells. Subcellular colocalization revealed

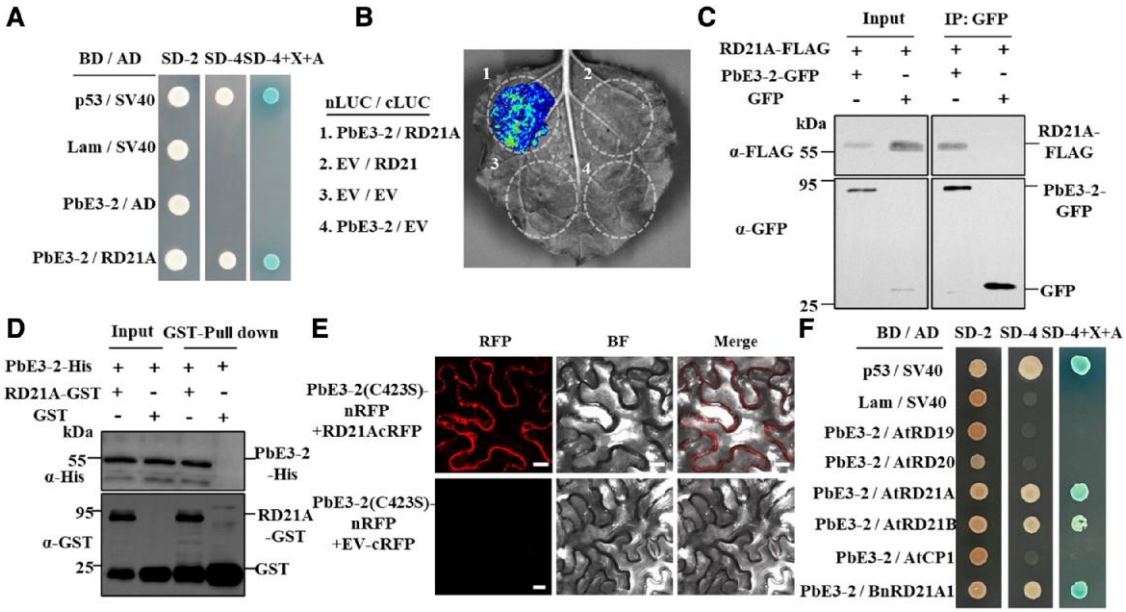

Figure 4. PbE3-2 interacts with *A. thaliana* cysteine protease RD21A. **A)** Y2H assays show that PbE3-2 interacts with RD21A. BD indicated pGBKT7 vector. BD indicates pGBKT7 vector. AD indicates pGADT7 vector. p53 + SV40 is a positive control, Lam + SV40 is a negative control. SD−Leu−Trp medium (SD-2) was used for screening clones harboring both plasmids and SD−Leu−Trp−His−Ade medium (SD-4) with/without X-a-Gal (X) and aureobasidin A **(A)** were used for verifying the interactions. **B)** Interaction between PbE3-2 and RD21A in split-LUC reconstitution assay. The constructs of N-terminal luciferase (nLUC) and C-terminal luciferase (cLUC) were coexpressed in *N. benthamiana* leaves. The combination containing the empty vector was used as a negative control. **C)** Co-IP confirmed that PbE3-2 interacts with RD21A in vivo. IP was performed with α-GFP agarose beads, followed by the detection of RD21 with α-FLAG antibody. Input and IP proteins were immunoblotted with α-FLAG and α-GFP antibodies. **D)** The direct interaction between PbE3-2 and RD21A was demonstrated by pull-down. Mixtures of PbE3-2-6 × His with GST-RD21A or GST were incubated with glutathione agarose beads for 3 h, and then the agarose beads were collected and washed 3 times and eluted. Immunoblotting of input and pull-down proteins was performed using α-His and α-GST antibodies. **E)** BiFC confirmed the interaction of PbE3-2 (C423S) and RD21A. PbE3-2 (C423S) is fused to the N-terminus of RFP; full-length RD21A is fused to the C-terminus of RFP. The corresponding GV3101 strains carrying the target plasmid are transiently expressed in the *N. benthamiana* and observed with a confocal laser-scanning microscope. Bars: 20 μm. Experiments were repeated twice with similar results. **F)** Y2H assays verified the specificity of PbE3-2 interaction with RD21A. PbE3-2 interacted with the *Arabidopsis* cysteine proteases AtRD21A (AT1G47128) and AtRD21B (AT5G43060) but not with the *Arabidopsis* cysteine proteases RESPONSIVE TO DEHYDRATION 19 (AtRD19) (AT4G39090) and AtCP1 (AT4G11310). PbE3-2 also did not interact with AtRD20 (AT2G33380). PbE3-2 interacted with RD21 homologs in *B. napus* (BnRD21A1 and BnaA08g04080D). Experiments in **A)**, **B)**, **C)**, **D)**, and **F)** were repeated 3 times with similar results.

that PbE3-2-GFP and RD21A-mCherry fluorescence signals were overlapped in the plasma membrane and cytoplasm (Supplemental Fig. S4C). This result is consistent with the localization of PbE3-2 (Supplemental Fig. S4B) and similar to the finding of Liu et al. (2020) that mature RD21A (mRD21A) interacts with the E3 ligase SINAT4 in the cytosol and plasma membrane. Taken together, these results suggest that PbE3-2 directly interacts with RD21A in vivo and in vitro.

Several RD21A-related genes were also cloned to examine the interaction with PbE3-2, including the cysteine proteases *AtRD19*, *AtRD21B*, and *cysteine protease 1* (*AtCP1*), RESPONSIVE TO DESSICATION 20 (*AtRD20*) from *A. thaliana*, and *BnRD21A1* from *Brassica napus*, an ortholog of *A. thaliana* AtRD21A. The results demonstrated that PbE3-2 interacts with AtRD21A, AtRD21B, and BnRD21A1 but not with AtRD19, AtRD20, and AtCP1 in yeast cells (Fig. 4F; Supplemental Fig. S6E). These results suggested that PbE3-2 interacts explicitly with cysteine proteases in the RD21 clade. Three orthologs of AtRD21A in rapeseed that can interact with PbE3-2 were examined by split-LUC complementation assays (Supplemental Fig. S5). The results demonstrated that the interactions between PbE3-2 and RD21 orthologs are conserved.

Full-length AtRD21A contains a signal peptide, an autoinhibitory precursor protein, a protease domain, a proline-rich region, and a granule protein domain (Yamada et al. 2001; Gu et al. 2012; Pogorelko et al. 2019). According to available information, this precursor protein has undergone extensive posttranslational processing, resulting in the formation of intermediate RD21A (iRD21A, removal of signal peptide and autoinhibitory prodomain) and mature/active RD21A (mRD21A, consisting of only the protease domain). To identify the structural requirements for the interaction between RD21A and PbE3-2, constructs of RD21A and its 4 truncated derivatives were used to analyze the potential interactions with PbE3-2 (Supplemental Fig. S6). PbE3-2 interacted with RD21A, iRD21A, mRD21A (Supplemental Fig. S6, C and E). Among the 4 constructs, the one containing the protease domain exhibited a stronger interaction with PbE3-2, suggesting that the protease domain of RD21A is responsible for

its interaction with PbE3-2. Besides, the granule protein domain had a much weaker interaction with PbE3-2 in the colony growth assay (Supplemental Fig. S6D) and thus is not essential to the interaction with PbE3-2. Split-LUC complementation imaging assays were performed to further verify the interactions between RD21A constructs and PbE3-2. All 3 forms of RD21A exhibited fluorescence (Supplemental Figs. S6B and S5C), indicating their interactions with PbE3-2 in vivo.

PbE3-2 ligase ubiquitinates RD21A

As PbE3-2 is an E3 ubiquitin ligase and interacts with RD21A, we investigated whether RD21A is a substrate of PbE3-2. We incubated recombinant AtUBA1-S (E1), PbE3-2-Myc, RD21A-HA, AtUBC8-S (E2), and His-FLAG-UBQ10 (ubiquitin) and tested for ubiquitination. The results revealed that RD21A was ubiquitinated by PbE3-2 with a laddering pattern and could not be ubiquitinated in the absence of any component of ubiquitin, E1, E2, or PbE3-2 (Fig. 5A). Besides, the PbE3-2 (C423S) mutant showed no self-ubiquitination and could not ubiquitinate RD21A (Fig. 5A), indicating that the cysteine residue at position 423 is essential for RD21A ubiquitination. Interestingly, the interaction of PbE3-2 and RD21A was not affected by the mutation (C423S) in the Y2H assay (Fig. 5B; Supplemental Fig. S6E), suggesting that the ubiquitin ligase activity of PbE3-2 is not required for the physical interaction between the 2 proteins. We then determined whether the other 2 forms of RD21A can be ubiquitinated by PbE3-2. The results showed that all 3 forms of RD21A, including full-length RD21A, iRD21A, and mRD21A, were ubiquitinated by PbE3-2 (Fig. 5C). Next, we investigated whether PbE3-2 facilitates RD21A degradation in plants. RD21A-FLAG was transiently coexpressed with PbE3-2-GFP or PbE3-2 (C423S)-GFP by *Agrobacterium* infiltration of *N. benthamiana*, and the protein level of RD21A-FLAG was assayed to assess whether it was degraded. RD21A showed increased protein levels when coexpressed with PbE3-2 (C423S) compared to that with PbE3-2, and the degradation of RD21A was inhibited by infiltration of the 26S proteasome degradation inhibitor MG132 (Fig. 5D). These results suggested that PbE3-2 directly ubiquitinates RD21A and results in its degradation via the 26S proteasome pathway.

RD21A ubiquitination sites

Since RD21A is ubiquitinated by PbE3-2, we predicted and identified the ubiquitination sites in RD21A protein sequences. We purified the ubiquitin-conjugated RD21A protein and identified the ubiquitination sites by MS analysis and identified 13 lysine sites (Supplemental Table S3). We then generated a dominant-negative ubiquitin mutant RD21A (K/R) with the substitution of the 13 predicted Lys (K) residues by Arg (R). As a result, the ubiquitination of RD21A (K/R) by PbE3-2 was substantially reduced compared with wild-type RD21A (Fig. 5E). To check whether some potential ubiquitination sites but not all of them are important for RD21A ubiquitination, we generated 4 single-site mutations, 1 double-site mutation, and 2 triple-site mutations of RD21A at K69, K260, K261, and K321, respectively. As shown in Supplemental Fig. S7, these mutations did not substantially reduce RD21A ubiquitination by PbE3-2 compared with wild-type RD21A, suggesting that RD21A may be polyubiquitinated by PbE3-2 at multiple Lys sites. We suspect that some of the potential ubiquitination sites are more important, but it is difficult to confirm at present. However, the interaction between PbE3-2 and RD21A (K/R) in yeast cells was not affected (Fig. 5F; Supplemental Fig. S6E). These results suggested that the 13 Lys residues in RD21A play an essential role in ubiquitination.

RD21A mediates plant disease resistance

To test whether RD21A contributes to resistance against *P. brassicae*, Col-0 and *rd21a* mutant plants were inoculated with *P. brassicae* for 21 d. The noninoculated *rd21a* mutant showed no morphological difference compared to Col-0 (Supplemental Fig. S2A). However, the inoculated *rd21a* mutant exhibited much more severe symptoms than Col-0 with yellow leaves and severe galling, while the control plants showed galls with lateral roots (Fig. 6A; Supplemental Fig. S2D). The percentage of severe galls (disease levels of 4 and 5) was 53% in Col-0 and 91% in *rd21a*. The disease index was 67.2 for Col-0 while 87.0 for *rd21a* (Fig. 6B). Quantification of *P. brassicae* biomass showed a significantly higher amount of *P. brassicae* in *rd21a* mutants than in Col-0 (Fig. 6, C and D). These results indicated that *rd21a* has reduced resistance to *P. brassicae* compared to Col-0. Besides, *rd21a* was more susceptible to *B. cinerea* than Col-0 (Supplemental Fig. S2, E and F). Since it is already known that PbE3-2 suppresses host defense response (Fig. 3), we tested whether RD21A mediates the defense response by comparing the ROS production, transcript levels of defense marker genes, and SA accumulation (Figs. 6, E and F, and 3D). Comparative analysis of chitin-triggered ROS burst, SA signaling pathway marker gene expression and SA accumulation revealed that they were substantially reduced in the *rd21a* mutant than in Col-0. However, there was no discernible difference between Col-0 and *rd21a* in the chitin-triggered MAPK activation (Supplemental Fig. S3B). Taken together, the *PbE3-2* transgenic plants and *rd21a* mutant had consistent disease susceptible phenotype and suppression of defense response, suggesting that PbE3-2 alters host defense responses by degrading plant RD21A protein through the 26S proteasome pathway, thereby promoting pathogen infection.

Role of PbE3s in *P. brassicae* pathogenesis

We next tested whether PbE3-3 and PbE3-4 perform the same function as PbE3-2. As a result, both of them were capable of self-ubiquitination (Supplemental Fig. S8A). In addition, PbE3-3 and PbE3-4 can suppress cell death induced by BAX in *N. benthamiana* (Supplemental Fig. S8B), suggesting that PbE3-3 and PbE3-4 can suppress plant immunity during the infection of host plants. In addition, PbE3-3 and

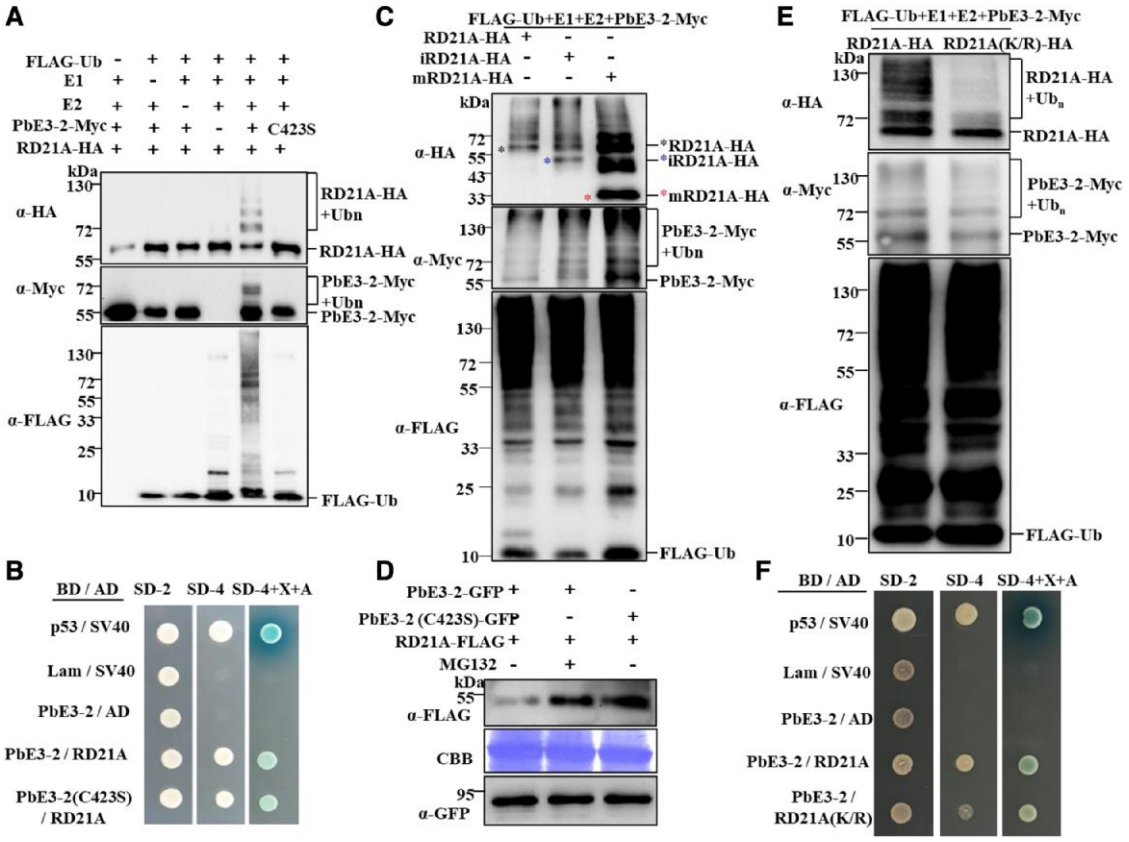

Figure 5. RD21A is a ubiquitinated substrate of PbE3-2 and is mediated by degradation through the 26S proteasome. **A)** PbE3-2 ubiquitinates RD21A whereas PbE3-2 (C423S), an enzyme active site mutant of PbE3-2, fails to ubiquitinate RD21A in the reconstituted system. **B)** Y2H assay shows that PbE3-2 (C423S), an enzyme active site mutant of PbE3-2, interacts with RD21A. **C)** RD21A, iRD21A, and mRD21A are ubiquitinated by PbE3-2 in the reconstituted system. **D)** PbE3-2 promotes the degradation of RD21A. *Agrobacterium* harboring RD21A-FLAG and PbE3-2-GFP or PbE3-2 (C423S)-GFP constructs were coinfiltrated in *N. benthamiana* leaves. Immunoblotting was performed with α-FLAG and α-GFP antibodies against RD21A and PbE3-2-GFP or PbE3-2 (C423S)-GFP, respectively. Protein loading was shown by Coomassie blue staining of Rubisco. **E)** Ubiquitination of RD21A (K/R) (13 Lys residues that identified as potential ubiquitination sites were mutated to Arg) by PbE3-2 was significantly reduced compared with wild-type RD21A. **F)** Y2H assay showing that RD21A(K/R), a ubiquitination site mutant of RD21A, interacts with PbE3-2. All experiments in Fig. 5 were repeated 3 times with similar results.

PbE3-4 associate with RD21A in a Y2H assay (Supplemental Figs. S8D and S6E). Interestingly, in the reconstituted ubiquitination system in *E. coli* cells, PbE3-3 and PbE3-4 also ubiquitinated RD21A (Supplemental Fig. S8C). RD21B is a homolog of RD21A with a 78.9% similarity at the amino acid level (Supplemental Fig. S9A) and also interacts with PbE3-2 (Fig. 4F; Supplemental Fig. S6E); therefore, they may be functionally redundant. To confirm this possibility, we determined whether RD21B is the substrate of these E3 ubiquitin ligases. As expected, we observed the ubiquitination of RD21B by PbE3-2 (Supplemental Fig. S9B).

Discussion

Plants have evolved complex innate immune systems to defend against various types of pathogens (Zhou and Zhang 2020). During infection, many eukaryotic biotrophic plant pathogens have evolved secretory proteins that in some cases avoid the immune perception and/or suppress immune responses to ensure successful infection (Toruno et al. 2016). *P. brassicae* is an obligate intracellular plant pathogen and has developed numerous effectors to promote infection (Pérez-López et al. 2018, 2020). Overexpression of *P. brassicae* effector PbBSMT in *Arabidopsis* promoted methyl-SA production and caused susceptibility to pathogens (Bulman et al. 2019). Overexpression of *P. brassicae* effector PBZF1 disrupted the expression of *Arabidopsis* SnRK1.1 regulation gene and enhanced *P. brassicae* virulence (Chen et al. 2021). Ubiquitination is involved in regulation of almost all cellular processes in eukaryotes. Many bacterial pathogens exploit host ubiquitin systems by delivering E3 ubiquitin ligase effector proteins or mimicking the E3 ubiquitin ligase to achieve successful infection (Ashida and Sasakawa 2017). An oomycete effector Avr1b interacts with soybean E3 ubiquitin ligase GmPUB1 to modulate host immunity (Li et al. 2021). A rice blast fungus effector avrpiz-t targets the RING-type E3 ubiquitin ligase APIP6 to suppress pathogen-associated molecular pattern-triggered immunity (Park et al. 2012).

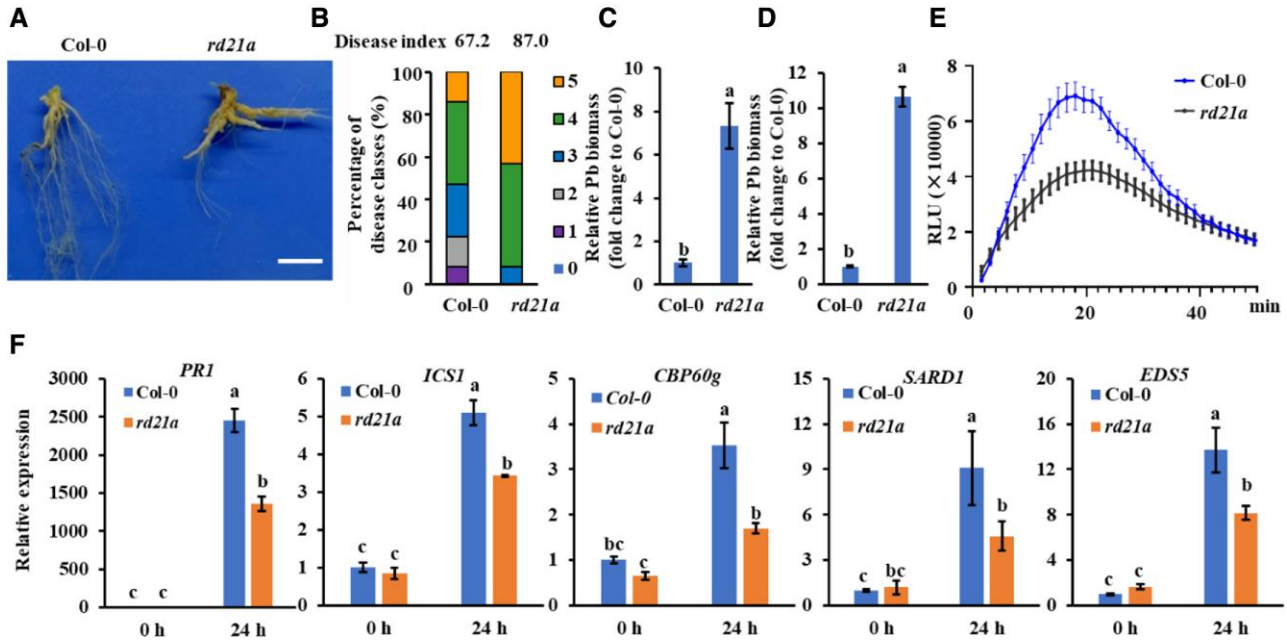

Figure 6. *Rd21a* mutants exhibit susceptibility to pathogens and reduced levels of immunity. **A)** Phenotype of Col-0 and *rd21a* at 21 d after *P. brassicae* inoculation. Bar: 1 cm. **B)** Disease index of Col-0 and *rd21a*. The percentages of plants in the individual disease classes are shown; Col-0 and *rd21a* used 35 to 40 plants for analysis. **C, D)** Quantification of *P. brassicae* content in diseased roots of *Arabidopsis* by qPCR, and the vertical coordinates indicate the multiplicity of *P. brassicae* content in different lines relative to Col-0. The relative biomass of *P. brassicae* is represented by the content of the *P. brassicae ACTIN* gene relative to that of the *Arabidopsis ACTIN2* gene **C)** and the content of the *P. brassicae DC1* gene relative to that of the Arabidopsis *GAPDH* gene **D)**. $n = 3$ biological replicates. A significant difference was determined by Student's *t*-test (2-tailed). Different letters (a and b) indicate significant differences. Data are shown as mean ± SD. **E)** Chitin-induced ROS burst is suppressed in *rd21a* mutant. The values represent means ± SE. $n = 16$ biological replicates. **F)** Induction of salicylate pathway genes was compromised in *rd21a* mutant. Leaves of 4-wk-old plants were infiltrated with 20-μg/mL chitin for 24 h. Data were normalized to *ACTIN2* expression in qPCR analysis. Statistical analysis was performed by 1-way ANOVA with Kruskal–Wallis test (significance set at $P \leq 0.05$). Different letters (a, b, and c) indicate significant differences. $n = 3$ biological replicates; data are shown as mean ± SD. Experiments in Fig. 6 were repeated 3 times with similar results.

PbRING1 was predicted to be a putative effector and display E3 ligase activity in vitro of *P. brassicae* in a previous study (Schwelm et al. 2015; Yu et al. 2019). In this study, PbE3-2, PbE3-3, and PbE3-4 were identified as secretory proteins, which are highly expressed in secondary infection and suppress cell death induced by BAX in *N. benthamiana*. These characteristics are consistent with the features of previously reported effectors (Chen et al. 2019; Pérez-López et al. 2020; Zhan et al. 2022). Hence, we suspect that they are candidate effectors. PbE3-2, PbE3-3, and PbE3-4 all harbor the RING domain at their C-terminus, which was found to have E3 ligase activity in vitro. Besides, PbE3-2, PbE3-3, and PbE3-4 can ubiquitinate RD21A and therefore may have the same biological functions. Bimolecular fluorescence complementation (BiFC) assay and colocalization assay indicated PbE3-2 interacts with RD21A in the plasma membrane and cytoplasm (Fig. 4F; Supplemental Fig. S4). Ubiquitination of RD21A by PbE3-2 may lead to poor fluorescence signals were detected in the BiFC assay (wild-type PbE3-2 and RD21A) and subcellular colocalization assay. Overall, our results suggested that *P. brassicae* secretes E3 ubiquitin ligases, taking the cruciferous cysteine protease RD21 as a virulence target and mediating its degradation to suppress plant immunity. Therefore, we propose a working model to summarize E3 ubiquitin ligases and RD21A-mediated immunity (Fig. 7). Here, we report on the functions of E3 ubiquitin ligase effectors in the pathogenesis of the mysterious protist *P. brassicae*.

RD21A was initially recognized as a drought-inducible gene (Koizumi et al. 1993). With the progress of relevant research, RD21A was found to play important roles in many biochemical processes, including plant immunity (Davies et al. 2015; Rustgi et al. 2017). RD21A is also involved in disease resistance of plants, including resistance to bacteria, fungi, and nematodes, and its mutation increases plant susceptibility (Shabab et al. 2008; Lozano-Torres et al. 2012; Shindo et al. 2012; Pogorelko et al. 2019; Liu et al. 2020). Proper RD21A homeostasis is critical as excessive accumulation of RD21A can lead to autoimmunity, while insufficient accumulation of RD21A may result in susceptibility to pathogens (Lampl et al. 2013; Boex-Fontvieille et al. 2015). Therefore, the level of RD21A in plant cells is tightly regulated by various biochemical reactions. In this study, we confirmed that knocking out *rd21a* resulted in higher susceptibility to *P. brassicae* (Fig. 6). ROS production and transcript levels of defense marker genes in the chitin-triggered immune responses substantially decreased in the *rd21a* plants than that in Col-0 (Fig. 6). Many biotrophic and necrotrophic plant pathogens regulate PTI by manipulating plant SA metabolism (Han and

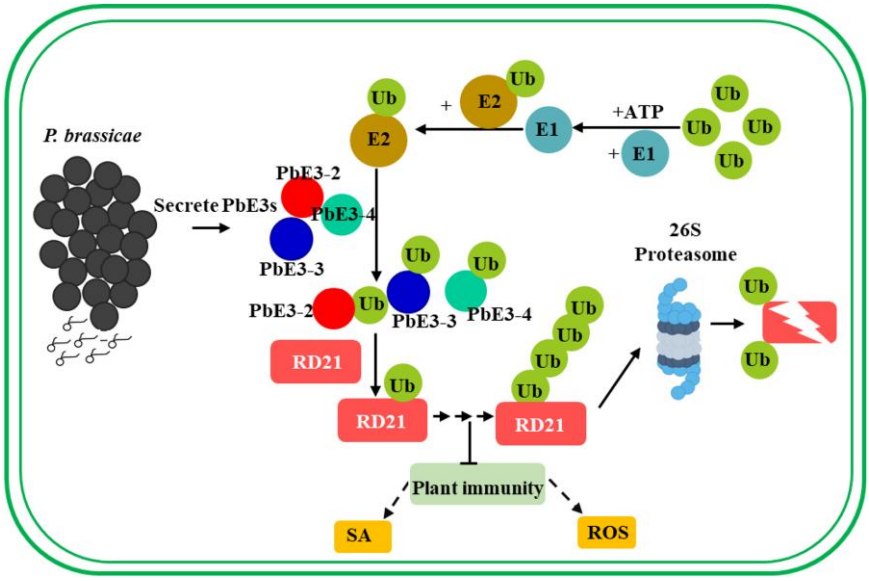

Figure 7. Working model of the mechanism for PbE3 to regulate plant immunity. E3 ubiquitin ligases secreted by *P. brassicae* directly target host cysteine protease RD21, leading to its degradation via the ubiquitin–proteasome pathway. Degradation of RD21, a positive regulator of plant immunity, leads to a reduction in the level of plant immunity and promotes infestation of *P. brassicae*. ROS, reactive oxygen species; SA, salicylic acid; Ub, ubiquitin.

Kahmann 2019; Chen et al. 2013). Application of exogenous SA suppresses clubroot disease in host, and SA-deficient mutants are more susceptible to the disease than the wild type (Chen et al. 2016). To counteract SA-related defenses, *P. brassicae* produces a methyltransferase effector PbBSMT to reduce SA content in the host cell and facilitate colonization and lead to clubroot disease (Ludwig-Müller et al. 2015; Djavaheri et al. 2019). In *PbE3-2* transgenic plants, the marker genes of the SA signaling pathway were suppressed and SA accumulation decreased under chitin treatment (Fig. 3). We suspect that results in susceptibility to *P. brassicae*. Although *S. sclerotiorum* is a necrotrophic fungal pathogen, at the early stages of infection, it grows in the apoplast without crossing the plant cell wall and the host cells are still alive at that stage (Kabbage et al. 2015). The defense against *S. sclerotiorum* in *Arabidopsis* and oilseed rape is also associated with SA signaling, and SA signaling pathway possibly acts as a positive regulator in plant immunity at the early stage of *S. sclerotiorum* infection (Yang et al. 2018; Tang et al. 2020). We speculate that the level of SA may be one of the reasons for the susceptibility of *PbE3-2* transgenic plants to *S. sclerotiorum*. Besides, RD21A played a crucial role in disease immunity, including resistance to fungi, nematodes, and bacteria. However, the mechanism by which RD21A regulates plant disease resistance is not well understood. In addition to SA, there may be ROS or other phytohormone, etc. In this study, PbE3-2 ubiquitinated and degraded RD21A, and the *rd21* mutant substantially decreased SA accumulation, which might contribute to the higher susceptibility of *PbE3-2* transgenic plants to the necrotrophic fungal pathogens than Col-0. It is necessary to clarify how RD21A manipulates plant SA metabolism will improve the understanding of the interaction between *P. brassicae* and the host. In addition, we still did not address whether PbE3-2-mediated immune responses defect dependent on RD21A. Because of the parasitic nature of the *P. brassicae*, it is currently almost impossible to obtain a knockout mutant of PbE3-2.

RD21A can be ubiquitinated by PbE3-2, PbE3-3, and PbE3-4 in vitro (Fig. 5; Supplemental Fig. S8). RD21B, a homolog of RD21A, can be ubiquitinated by PbE3-2 (Supplemental Fig. S9). All these results suggest the ubiquitination of RD21 by secreted E3 ubiquitin ligase in *P. brassicae*. In previous reports, RD21A level was also regulated by the plant ubiquitination system (Kim and Kim 2013). RD21A can interact with the ubiquitin E3 ligase SINAT4 to participate in drought-induced immunity (Liu et al. 2020). Different from previous reports, we identified that pathogen secreted E3 ligase to regulate the RD21A level. We also identified 13 potential ubiquitination sites on RD21A and generated the RD21A ubiquitination site mutant RD21AK/R. The ubiquitination of RD21AK/R by PbE3-2 was much less substantial than that of wild-type RD21A. However, it is interesting to identify the real ubiquitination sites. Unfortunately, the 7 generated mutations resulted in no substantial reduction in the ubiquitination of RD21A compared with RD21AK/R. It is possible that some of them are important ubiquitination sites, but they are difficult to be identified as there are many combinations. It remains to be determined whether substituting arginine for the 13 Lys residues of RD21A would perturb its degradation in vivo in future work. The PLCPs have important, complex and not fully understood functions for the regulation of plant immunity. PLCPs contribute to plant resistance to widespread pathogens. Tomato immune proteases RCR3 and PIP1 are involved in resistance to fungal and oomycete

pathogens (Rooney et al. 2005; Kaschani et al. 2010; Paulus et al. 2020). Maize immune signaling peptide 1 (Zip1) is released by PLCP and can strongly trigger the accumulation of SA in leaves (Ziemann et al. 2018). OsXCP2, a PLCP in rice, mediates resistance against *Xanthomonas oryzae* by elevating SA levels and ROS accumulation (Niño et al. 2020). In addition, protease could split microbial peptides to trigger immune responses (Wang et al. 2021). Since PLCP plays an important role in plant immunity, many pathogens secrete effector to target PLCP. Huanglongbing-associated pathogen secreting SDE1 directly interacts with citrus PLCP and inhibits its protease activity (Clark et al. 2018). *P. syringae* secretes CIP1 to inhibit tomato immune-associated protease thereby promoting virulence (Shindo et al. 2016). The cyst nematode effector Hs4E02 targets plant defense protease and achieves virulence by altering its subcellular localization (Pogorelko et al. 2019). In the present study, we identified *P. brassicae* directly targets the plant defense-associated cysteine protease RD21A to promote virulence, which increases our understanding of the pathogenesis of protist. Therefore, future studies of how RD21A regulates plant resistance to *P. brassicae* are of relevance. In the future, RD21A may be genetically edited to help plants breed against clubroot disease.

In summary, our results suggest that the cysteine protease RD21 is a positive regulator of plant immunity and that *P. brassicae* secretes E3 ubiquitin ligases to directly target RD21 for degradation, thereby weakening plant immunity for successful infection. This study may help the generation of germplasm with higher clubroot resistance in the future.

Materials and methods

P. brassicae inoculation

P. brassicae strain ZJ-1 was isolated by Chen et al. (2016). *P. brassicae* resting spores were collected from the galls and kept at 4 °C. One milliliter of 1.0×10^7 spores/mL resting spore suspension was inoculated onto 14-d-old *Arabidopsis* (*A. thaliana*) seedlings through the soil around the roots, followed by 21 dpi analysis. A modified 0 to 5 scoring system from previous studies was used to assess disease severity (Siemens et al. 2012): 0, no disease; 1, extremely little galls primarily on lateral roots, with negligible harm to main roots; 2, the main roots and a few lateral roots were covered in tiny galls; 3, main root with medium to large globules; 4, severe galls on lateral roots, main roots or rosettes, with total fine root damage on lateral roots; and 5, completely expansion and rotting of roots.

Plants and growth conditions

The *Arabidopsis* and *N. benthamiana* plants were grown in greenhouse at 12-h day, 12-h night, 22 °C, and 60% relative humidity. The *rd21a* mutant was obtained using the CRISPR/Cas9 method in a Col-0 background (Liu et al. 2020). *PbE3-2* transgenic *A. thaliana* line was generated by using *Agrobacterium* (*A. tumefaciens*)-mediated transformation by floral dipping (Clough and Bent 1998).

Yeast invertase secretion assay

PbE3-2-SP was cloned into the vector pSUC2. The pSUC2, pSUC2-avr1b-SP (positive control), and pSUC2-PbE3-2-SP fusion vectors were transformed into yeast (*S. cerevisiae*) strain YTK12. The transformants were grown on CMD-W (0.67% [w/v] yeast N base without amino acids, Trp dropout supplement, 2% [w/v] sucrose, 0.1% [w/v] glucose, and 2% [w/v] agar) or YPRAA medium (1% [w/v] yeast extract, 2% [w/v] peptone, 2% [w/v] raffinose, 2-μg/L antimycin A, and 2% [w/v] agar) for invertase secretion assays. Invertase enzymatic activity was detected by the reduction of 2,3,5-triphenyltetrazolium chloride (TTC) to red-colored insoluble triphenylformazan.

Apoplastic fluid assay

Extraction of plasmatic extracellular fluid was conducted according to a previous protocol (O'Leary et al. 2014). Sterile water was infiltrated by a vacuum pump into the leaves of *N. benthamiana* with transient expression of PbE3-2 or PbE3-$2^{\Delta SP}$ protein. The apoplast washing fluid was recovered by centrifugation and concentrated for western blotting to verify that proteins were secreted into the apoplast.

Confocal microscopy assay

For subcellular localization or BiFC assay, *A. tumefaciens* strain GV3101 carrying the desired constructs was infiltrated into *N. benthamiana* leaves; GFP, YFP, or RFP fluorescence signals were examined at 2 to 3 dpi with confocal microscopy (Nikon, A1HD25). GFP or YFP was detected after excitation with a 488-nm wavelength laser, and emissions were collected between 500 and 550 nm. RFP was detected after excitation with a 561-nm wavelength laser, and emissions were collected between 570 and 620 nm. Laser intensity is in the range of 2.0 to 3.0, and gain is in the range of 50 to 80.

Ubiquitination assay

Ubiquitination assay was performed by reconstituted ubiquitination reactions in *E. coli* (Han et al. 2017). *Arabidopsis* ubiquitin UBQ10 was constructed into the prokaryotic expression vector pET28a. AtUBA1 and RD21A were constructed into the compatible dual expression vector pCDFDuet, and AtUBC8 and PbE3-2 were constructed into the compatible dual expression vector pACYDuet. Strains lacking any of these components were used as negative controls. Self-ubiquitination reactions were performed with strains lacking the substrate. Western blot of purified proteins from crushed organisms was performed to determine the occurrence of ubiquitination according to the previous method.

Measurement of the amount of *P. brassicae* DNA in diseased roots

Extraction of DNA from infected roots was performed using the cetyltrimethylammonium bromide method (Allen et al. 2006). qPCR was performed as described by Chen et al. (2016). The relative biomass of *P. brassicae* is represented by the content of the *P. brassicae ACTIN* gene (AY452179.1)

relative to that of the *Arabidopsis ACTIN2* gene (AT3G18780), or the content of *P. brassicae* is represented by the content of the *P. brassicae DC1* gene from a partial 18S rRNA gene sequence (AF231027) relative to that of the *Arabidopsis GAPDH* gene (AT1G13440) (Rennie et al. 2011). The qPCR primers used are listed in Supplemental Table S4.

ROS assay and MAPK assay

ROS assay and MAPK assay were conducted as previously described (Qi et al. 2022). *Arabidopsis* leaf discs from 4-wk-old plants after overnight incubation with ddH_2O were treated with 100-μL solution containing 5 μM L-012 (Wako, 120-04891, Japan), 10-μg/mL horseradish peroxidase (Sigma, P6782, USA), and 20-μg/mL chitin. ROS production was measured using a Multimode Reader Platform (Tecan Austria GmbH, SPARK 10M) with a reading interval of 1.5 and 50 min per treatment. Five leaf discs were transferred to 6-well plates with H_2O overnight and then treated with 20-μg/mL chitin for 5, 15, or 30 min, respectively. Used α-pErk1/2 antibody (Cell Signaling Technology, 9101, USA) to detect the level of pMPK3 and pMPK6.

IP and LC-MS analysis

The IP experiment was performed as previously described (Yang et al. 2018), using IP buffer (Beyotime, P0013, China) to extract the total protein from *PbE3-2-GFP* transgenic plants. About 50 mL of protein extract was incubated with 100 μL of α-GFP agarose beads (ChromoTek, gta-20, Germany) for 12 h at 4 °C. Beads were collected by centrifugation at 1,000 × *g* for 1 min at 4 °C, washed with 1 mL of IP buffer 3 times, and boiled for 5 min to elute the bound proteins from the beads. The proteins were sent to HOOGEN BIOTECH Company (Shanghai, China) for LC-MS analysis (Q Exactive, Thermo Fisher).

Y2H system

The cDNA encoding the PbE3-2 without signal peptide was cloned into pGBKT7 vector, and the candidate proteins identified from LC-MS were constructed into pGADT7. Both plasmids were transformed into Y2H golden yeast cells using polyethylene glycol/LiAc-mediated yeast transformation. The transformation mix was spread on SD medium−Leu−Trp (SD-2, selects for both plasmids), and positive clones were further confirmed on SD medium−Trp−Leu−His−Ade (SD-4) containing X-α-Gal and aureobasidin A.

Co-IP assay

Transient expression of RD21A-FLAG with PbE3-2-GFP or GFP was performed in *N. benthamiana* by *Agrobacterium* infiltration. Extraction of total proteins with IP buffer was followed by IP with α-GFP agarose beads (ChromoTek, gta-20, Germany) at 4 °C for 1 h. Beads were collected, washed 3 times with IP buffer, and immunoblotted with α-FLAG antibody.

Split-LUC complementation assay

The split-LUC reconstitution assay was carried out as previously reported (Chen et al. 2008). Different N-terminal luciferase (nLUC) or C-terminal luciferase (cLUC) constructs were introduced into *A. tumefaciens* strain GV3101. *Agrobacterium* suspension (OD_{600} = 1.5) carrying the specified nLUC and cLUC plasmids was coinfiltrated into 4-wk-old *N. benthamiana* leaves. About 1 mM luciferin (YEASEN, 40901ES01, China) was infiltrated 48 h after infiltration, and luminescence was imaged within 5 min using a charge-coupled device imaging apparatus.

Western blots

Western blot was carried out as previously described (Chen et al. 2012). Proteins were separated by 10% SDS–PAGE and transferred to 0.2-μm PVDF membranes for 1 h. In each experiment, a parallel gel was stained with Coomassie brilliant blue as a loading control. The following antibodies were used: mouse anti-FLAG (Sigma Aldrich) at a 1:2,000 dilution, mouse anti-GFP (ABclonal) at a 1:2,000 dilution, rabbit anti-HA (ABclonal) at a 1:2,000 dilution, mouse anti-GST (ABclonal) at a 1:2,000 dilution, mouse anti-His (ABclonal) at a 1:2,000 dilution, mouse anti-Myc (Genscript) at a 1:2,000 dilution, HRP-conjugated anti-rabbit IgG secondary antibodies (ABclonal) at a 1:10,000 dilution, and HRP-conjugated anti-mouse IgG secondary antibodies (ABclonal) at a 1:10,000 dilution.

SA extraction and quantification

SA was extracted and quantified as previously described with some modifications (Huot et al. 2017). Four-week-old *Arabidopsis* leaves were infiltrated with 20 μg/mL of chitin or water, and 24 h after infiltration, leaf tissue between 50 and 100 mg (fresh weight) was flash-frozen in liquid nitrogen, ground, and extracted at 4 °C with extraction buffer. Filtered extracts were quantified using an ultrafast LC-electrospray ionization tandem MS as previously described (Liu et al. 2012).

Accession numbers

Sequence data from this article can be found in the GenBank/EMBL data libraries under accession numbers: PbE3-1, ON394060; PbE3-2, ON394061; PbE3-3, ON394062; PbE3-4, ON394063; PbE3-5, ON394064; RD21A, NP_564497.1; RD21B, NP_568620.1; RD19, NP_568052.1; RD20, NP_180896.1; CP1, NP_567376.1; BnRD21A1, CDY17044.1; BnRD21A2, CDY17093.1; and BnRD21A3, CDY06760.1.

Acknowledgments

We thank Dr. Yi Liu from the Chinese Academy of Sciences for the seeds of *rd21a* mutant. We thank Dr. Dongping Lu from the Institute of Genetics and Developmental Biology for sharing the in vitro ubiquitination assay system. We thank Dr. Yangrong Cao from Huazhong Agricultural University for sharing the split-LUC vectors. We thank Dr. Shuai Fang and

Hongbo Liu for providing technical support on SA quantification. We thank Dr. Kenichi Tsuda, Shengyang He, and Kabin Xie for their critical reading of the manuscript and constructive suggestions. We thank research associates at the Center for Protein Research (CPR), Huazhong Agricultural University, for the technical support. We would like to thank the State Key Laboratory of Agricultural Microbiology Core Facility for the assistance in confocal microscopy.

Author contributions

C.L. and T.C. conceived the project and designed experiments. C.L. performed most of the experiments. C.L., S. L., L.F., and Q. W. performed experiments and analyzed the data. J.C., J.X., Y.L., Y.F., and D.J. analyzed the data and provided advice that helped shape the research. C.L. and T.C. wrote the manuscript with input from all coauthors.

Supplemental data

The following materials are available in the online version of this article.

Supplemental Figure S1. Analysis of secreted PbE3s.

Supplemental Figure S2. Growth phenotype of Col-0, *PbE3-2* overexpression plants, and *rd21a* mutant.

Supplemental Figure S3. Chitin triggered *RBOHD* gene expression and MAPK activation in *PbE3-2* overexpression lines.

Supplemental Figure S4. BiFC on the interaction between PbE3-2 with RD21A in planta, subcellular localization of PbE3-2, and subcellular colocalization of PbE3-2 and RD21A.

Supplemental Figure S5. PbE3-2 interacts with *B. napus* BnRD21A.

Supplemental Figure S6. PbE3-2 interacts with truncated RD21A.

Supplemental Figure S7. Detection the ubiquitination sites of RD21A by PbE3-2.

Supplemental Figure S8. PbE3-2, PbE3-3, and PbE3-4 interacted with RD21, respectively.

Supplemental Figure S9. PbE3-2 ubiquitinate RD21A and RD21B, respectively.

Supplemental Table S1. The information of E3 ubiquitin ligases in the genome of *P. brassicae* ZJ-1.

Supplemental Table S2. List of potential PbE3-2 interacting partners identified by IP-MS/MS analysis.

Supplemental Table S3. Ubiquitination sites by LC-MS.

Supplemental Table S4. Primers used in the study.

Funding

This research was financially supported by the National Natural Science Foundation of China (32172371), the Fundamental Research Funds for the Central Universities (2662023PY006), the earmarked fund of China Agriculture Research System (CARS-12), and the collaborative fund of Huazhong Agricultural University and Agricultural Genomics Institute at Shenzhen (SZYJY2021007).

Conflict of interest statement. None declared.

Data availability

The data are available on request from the corresponding author.

References

Abramovitch RB, Janjusevic R, Stebbins CE, Martin GB. Type III effector AvrPtoB requires intrinsic E3 ubiquitin ligase activity to suppress plant cell death and immunity. Proc Natl Acad Sci U S A. 2006:**103**(8):2851–2856. https://doi.org/10.1073/pnas.0507892103

Allen GC, Flores-Vergara MA, Krasynanski S, Kumar S, Thompson WF. A modified protocol for rapid DNA isolation from plant tissues using cetyltrimethylammonium bromide. Nat Protoc. 2006:**1**(5):2320–2325. https://doi.org/10.1038/nprot.2006.384

Ashida H, Sasakawa C. Bacterial E3 ligase effectors exploit host ubiquitin systems. Curr Opin Microbiol. 2017:**35**:16–22. https://doi.org/10.1016/j.mib.2016.11.001

Bi K, Chen T, He Z, Gao Z, Zhao Y, Liu H, Fu Y, Xie J, Cheng J, Jiang D, et al. Comparative genomics reveals the unique evolutionary status of *Plasmodiophora brassicae* and the essential role of GPCR signaling pathways. Phytopathol Res. 2019:**12**:1. https://doi.org/10.1186/s42483-019-0018-6

Bi K, He Z, Gao Z, Zhao Y, Fu Y, Cheng J, Xie J, Jiang D, Chen T. Integrated omics study of lipid droplets from *Plasmodiophora brassicae*. Sci Rep. 2016:**6**(1):36965. https://doi.org/10.1038/srep36965

Boex-Fontvieille E, Rustgi S, Reinbothe S, Reinbothe C. A Kunitz-type protease inhibitor regulates programmed cell death during flower development in *Arabidopsis thaliana*. J Exp Bot. 2015:**66**(20):6119–6135. https://doi.org/10.1093/jxb/erv327

Bulman S, Richter F, Marschollek S, Benade F, Jülke S, Ludwig-Müller J. *Arabidopsis thaliana* expressing PbBSMT, a gene encoding a SABATH-type methyltransferase from the plant pathogenic protist *Plasmodiophora brassicae*, show leaf chlorosis and altered host susceptibility. Plant Biol (Stuttg). 2019:**1**(Suppl 1):120–130. https://doi.org/10.1111/plb.12728

Chen T, Bi K, He Z, Gao Z, Zhao Y, Fu Y, Cheng J, Xie J, Jiang D. *Arabidopsis* mutant bik1 exhibits strong resistance to *Plasmodiophora brassicae*. Front Physiol. 2016:**7**:402. https://doi.org/10.3389/fphys.2016.00402

Chen W, Li Y, Yan R, Ren L, Liu F, Zeng L, Sun S, Yang H, Chen K, Xu L, et al. SnRK1.1-mediated resistance of *Arabidopsis thaliana* to clubroot disease is inhibited by the novel *Plasmodiophora brassicae* effector PBZF1. Mol Plant Pathol. 2021:**22**(9):1057–1069. https://doi.org/10.1111/mpp.13095

Chen W, Li Y, Yan R, Xu L, Ren L, Liu F, Zeng L, Yang H, Chi P, Wang X, et al. Identification and characterization of *Plasmodiophora brassicae* primary infection effector candidates that suppress or induce cell death in host and nonhost plants. Phytopathology. 2019:**109**(10):1689–1697. https://doi.org/10.1094/PHYTO-02-19-0039-R

Chen PW, Singh P, Zimmerli L. Priming of the *Arabidopsis* pattern-triggered immunity response upon infection by necrotrophic *Pectobacterium carotovorum* bacteria. Mol Plant Pathol. 2013:**14**(1):58–70. https://doi.org/10.1111/j.1364-3703.2012.00827.x

Chen T, Zhu H, Ke DX, Cai K, Wang C, Gou HL, Hong ZL, Zhang ZM. A MAP kinase kinase interacts with SymRK and regulates nodule organogenesis in *Lotus japonicus*. Plant Cell. 2012:**24**(2):823–838. https://doi.org/10.1105/tpc.112.095984

Chen H, Zou Y, Shang Y, Lin H, Wang Y, Cai R, Tang X, Zhou JM. Firefly luciferase complementation imaging assay for protein-protein interactions in plants. Plant Physiol. 2008:**146**(2):368–376. https://doi.org/10.1104/pp.107.111740

Clark K, Franco JY, Schwizer S, Pang Z, Hawara E, Liebrand TWH, Pagliaccia D, Zeng L, Gurung FB, Wang P, et al. An effector from the Huanglongbing-associated pathogen targets citrus proteases. Nat Commun. 2018:**9**(1):1718. https://doi.org/10.1038/s41467-018-04140-9

Clough SJ, Bent AF. Floral dip: a simplified method for *Agrobacterium*-mediated transformation of *Arabidopsis thaliana*. Plant J. 1998:**16**(6):735–743. https://doi.org/10.1046/j.1365-313x.1998.00343.x

Davies LJ, Lei Z, Axel AA. The *Arabidopsis thaliana* papain-like cysteine protease RD21 interacts with a root-knot nematode effector protein. Nematology. 2015:**17**(6):655–666. https://doi.org/10.1163/15685411-00002897

Devendrakumar KT, Li X, Zhang YL. MAP kinase signalling: interplays between plant PAMP- and effector-triggered immunity. Cell Mol Life Sci. 2018:**75**(16):2981–2989. https://doi.org/10.1007/s00018-018-2839-3

Djavaheri M, Ma LS, Klessig DF, Mithofer A, Gropp G, Borhan H. Mimicking the host regulation of salicylic acid: a virulence strategy by the clubroot pathogen *Plasmodiophora brassicae*. Mol Plant Microbe Interact. 2019:**32**(3):296–305. https://doi.org/10.1094/MPMI-07-18-0192-R

Dodds PN, Rathjen JP. Plant immunity: towards an integrated view of plant–pathogen interactions. Nat Rev Genet. 2010:**11**(8):539–548. https://doi.org/10.1038/nrg2812

Fang S, Weissman AM. A field guide to ubiquitylation. Cell Mol Life Sci. 2004:**61**(13):1546–1561. https://doi.org/10.1007/s00018-004-4129-5

Galindo-González L, Manolii V, Hwang SF, Strelkov SE. Response of *Brassica napus* to *Plasmodiophora brassicae* involves salicylic acid-mediated immunity: an RNA-seq-based study. Front Plant Sci. 2020:**11**:1025. https://doi.org/10.3389/fpls.2020.01025

Gu C, Shabab M, Strasser R, Wolters PJ, Shindo T, Niemer M, Kaschani F, Mach L, van der Hoorn RA. Post-translational regulation and trafficking of the granulin-containing protease RD21 of *Arabidopsis thaliana*. PLoS One. 2012:**7**(3):e32422. https://doi.org/10.1371/journal.pone.0032422

Guo Y, Li B, Li M, Zhu H, Yang Q, Liu X, Qu L, Fan L, Wang T. Efficient marker-assisted breeding for clubroot resistance in elite Pol-CMS rapeseed varieties by updating the PbBa8.1 locus. Mol Breed. 2022:**42**(7):41. https://doi.org/10.1007/s11032-022-01305-9

Han XW, Kahmann R. Manipulation of phytohormone pathways by effectors of filamentous plant pathogens. Front Plant Sci. 2019:**10**:822. https://doi.org/10.3389/fpls.2019.00822

Han Y, Sun J, Yang J, Tan Z, Luo J, Lu D. Reconstitution of the plant ubiquitination cascade in bacteria using a synthetic biology approach. Plant J. 2017:**91**(4):766–776. https://doi.org/10.1111/tpj.13603

Hershko A, Ciechanover A. The ubiquitin system. Annu Rev Biochem. 1998:**67**(1):425–479. https://doi.org/10.1146/annurev.biochem.67.1.425

Huot B, Castroverde CDM, Velasquez AC, Hubbard E, Pulman JA, Yao J, Childs KL, Tsuda K, Montgomery BL, He SY. Dual impact of elevated temperature on plant defence and bacterial virulence in *Arabidopsis*. Nat Commun. 2017:**8**(1):1808. https://doi.org/10.1038/s41467-017-01674-2

Hwang SF, Strelkov SE, Feng J, Gossen BD, Howard RJ. *Plasmodiophora brassicae*: a review of an emerging pathogen of the Canadian canola (*Brassica napus*) crop. Mol Plan Pathol. 2012:**13**(2):105–113. https://doi.org/10.1111/j.1364-3703.2011.00729.x

Javed MA, Schwelm A, Zamani-Noor N, Salih R, Vano MS, Wu JX, Garcia MG, Heick TM, Luo CY, Prakash P, et al. The clubroot pathogen *Plasmodiophora brassicae*: a profile update. Mol Plant Pathol. 2023:**24**(2):89–106. https://doi.org/10.1111/mpp.13283

Kabbage M, Yarden O, Dickman MB. Pathogenic attributes of *Sclerotinia sclerotiorum*: switching from a biotrophic to necrotrophic lifestyle. Plant Sci. 2015:**233**:53–60. https://doi.org/10.1016/j.plantsci.2014.12.018

Kaschani F, Shabab M, Bozkurt T, Shindo T, Schornack S, Gu C, Ilyas M, Win J, Kamoun S, van der Hoorn RA. An effector-targeted protease contributes to defense against *Phytophthora infestans* and is under diversifying selection in natural hosts. Plant Physiol. 2010:**154**(4):1794–1804. https://doi.org/10.1104/pp.110.158030

Kim JM, Cho EN, Kwon YE, Bae SJ, Kim M, Seol JH. CHFR functions as a ubiquitin ligase for HLTF to regulate its stability and functions. Biochem Biophys Res Commun. 2010:**395**(4):515–520. https://doi.org/10.1016/j.bbrc.2010.04.052

Kim JH, Kim WT. The *Arabidopsis* RING E3 ubiquitin ligase AtAIRP3/LOG2 participates in positive regulation of high-salt and drought stress responses. Plant Physiol. 2013:**162**(3):1733–1749. https://doi.org/10.1104/pp.113.220103

Koizumi M, Yamaguchi-Shinozaki K, Tsuji H, Shinozaki K. Structure and expression of two genes that encode distinct drought-inducible cysteine proteinases in *Arabidopsis thaliana*. Gene. 1993:**129**(2):175–182. https://doi.org/10.1016/0378-1119(93)90266-6

Kong L, Cheng J, Zhu Y, Ding Y, Meng J, Chen Z, Xie Q, Guo Y, Li J, Yang S, et al. Degradation of the ABA co-receptor ABI1 by PUB12/13 U-box E3 ligases. Nat Commun. 2015:**6**(1):8630. https://doi.org/10.1038/ncomms9630

Lampl N, Alkan N, Davydov O, Fluhr R. Set-point control of RD21 protease activity by AtSerpin1 controls cell death in *Arabidopsis*. Plant J. 2013:**74**(3):498–510. https://doi.org/10.1111/tpj.12141

Li S, Hanlon R, Wise H, Pal N, Brar H, Liao CY, Gao HY, Perez E, Zhou LC, Tyler BM, et al. Interaction of *Phytophthora sojae* effector Avr1b with E3 ubiquitin ligase GmPUB1 is required for recognition by soybeans carrying *Phytophthora* resistance *Rps1-b* and *Rps1-k* genes. Front Plant Sci. 2021:**12**:725571. https://doi.org/10.3389/fpls.2021.725571

Liu HB, Li XH, Xiao JH, Wang SP. A convenient method for simultaneous quantification of multiple phytohormones and metabolites: application in study of rice–bacterium interaction. Plant Methods. 2012:**8**(1):2. https://doi.org/10.1186/1746-4811-8-2

Liu Y, Wang K, Cheng Q, Kong D, Zhang X, Wang Z, Wang Q, Xie Q, Yan J, Chu J, et al. Cysteine protease RD21A regulated by E3 ligase SINAT4 is required for drought-induced resistance to *Pseudomonas syringae* in *Arabidopsis*. J Exp Bot. 2020:**71**(18):5562–5576. https://doi.org/10.1093/jxb/eraa255

Lozano-Torres JL, Wilbers RH, Gawronski P, Boshoven JC, Finkers-Tomczak A, Cordewener JH, America AH, Overmars HA, Van 't Klooster JW, Baranowski L, et al. Dual disease resistance mediated by the immune receptor Cf-2 in tomato requires a common virulence target of a fungus and a nematode. Proc Natl Acad Sci U S A. 2012:**109**(25):10119–10124. https://doi.org/10.1073/pnas.1202867109

Lu D, Lin W, Gao X, Wu S, Cheng C, Avila J, Heese A, Devarenne TP, He P, Shan L. Direct ubiquitination of pattern recognition receptor FLS2 attenuates plant innate immunity. Science. 2011:**362**(6036):1439–1442. https://doi.org/10.1126/science.1204903

Ludwig-Müller J, Jülke S, Geiß K, Richter F, Mithöfer A, Šola I, Rusak G, Keenan S, Bulman S. A novel methyltransferase from the intracellular pathogen *Plasmodiophora brassicae* methylates salicylic acid. Mol Plant Pathol. 2015:**16**(4):349–364. https://doi.org/10.1111/mpp.12185

Melotto M, Underwood W, Koczan J, Nomura K, He SY. Plant stomata function in innate immunity against bacterial invasion. Cell. 2006:**126**(5):969–980. https://doi.org/10.1016/j.cell.2006.06.054

Niño MC, Kang KK, Cho YG. Genome-wide transcriptional response of papain-like cysteine protease-mediated resistance against *Xanthomonas oryzae* pv. oryzae in rice. Plant Cell Rep. 2020:**39**:457–472.

O'Leary BM, Rico A, McCraw S, Fones HN, Preston GM. The infiltration-centrifugation technique for extraction of apoplastic fluid from plant leaves using *Phaseolus vulgaris* as an example. J Vis Exp. 2014:**94**:52113. https://doi.org/10.3791/52113

Park CH, Chen S, Shirsekar G, Zhou B, Khang CH, Songkumarn P, Afzal AJ, Ning Y, Wang R, Bellizzi M, et al. The *Magnaporthe oryzae* effector AvrPiz-t targets the RING E3 ubiquitin ligase APIP6 to suppress pathogen-associated molecular pattern-triggered immunity

in rice. Plant Cell. 2012:**24**(11):4748–6472. https://doi.org/10.1105/tpc.112.105429

Park CH, Shirsekar G, Bellizzi M, Chen S, Songkumarn P, Xie X, Shi X, Ning Y, Zhou B, Suttiviriya P, et al. The E3 ligase APIP10 connects the effector AvrPiz-t to the NLR receptor Piz-t in rice. PLoS Pathog. 2016:**12**(3):e1005529. https://doi.org/10.1371/journal.ppat.1005529

Paulus JK, Kourelis J, Ramasubramanian S, Homma F, Godson A, Hörger AC, Hong TN, Krahn D, Ossorio Carballo L, Wang S, et al. Extracellular proteolytic cascade in tomato activates immune protease Rcr3. Proc Natl Acad Sci U S A. 2020:**117**(29):17409–17417. https://doi.org/10.1073/pnas.1921101117

Peng YJ, van Wersch R, Zhang YL. Convergent and divergent signaling in PAMP-triggered immunity and effector-triggered immunity. Mol Plant Microbe Interact. 2018:**31**(4):403–409. https://doi.org/10.1094/MPMI-06-17-0145-CR

Pérez-López E, Hossain MM, Tu JY, Waldner M, Todd CD, Kusalik AJ, Wei YD, Bonham-Smith PC. Transcriptome analysis identifies *Plasmodiophora brassicae* secondary infection effector candidates. J Eukaryot Microbiol. 2020:**67**(3):337–351. https://doi.org/10.1111/jeu.12784

Pérez-López E, Hossain MM, Wei Y, Todd CD, Bonham-Smith PC. A clubroot pathogen effector targets cruciferous cysteine proteases to suppress plant immunity. Virulence. 2021:**12**(1):2327–2340. https://doi.org/10.1080/21505594.2021.1968684

Pérez-López E, Waldner M, Hossain M, Kusalik AJ, Wei Y, Bonham-Smith PC, Todd CD. Identification of *Plasmodiophora brassicae* effectors—a challenging goal. Virulence. 2018:**9**(1):1344–1353. https://doi.org/10.1080/21505594.2018.1504560

Pogorelko GV, Juvale PS, Rutter WB, Hütten M, Maier TR, Hewezi T, Paulus J, van der Hoorn RA, Grundler FM, Siddique S, et al. Re-targeting of a plant defense protease by a cyst nematode effector. Plant J. 2019:**98**(6):1000–1014. https://doi.org/10.1111/tpj.14295

Qi P, Huang M, Hu X, Zhang Y, Wang Y, Li P, Chen S, Zhang D, Cao S, Zhu W, et al. A *Ralstonia solanacearum* effector targets TGA transcription factors to subvert salicylic acid signaling. Plant Cell. 2022:**34**(5):1666–1683. https://doi.org/10.1093/plcell/koac015

Rennie DC, Manolii VP, Cao T, Hwang SF, Howard RJ, Strelkov SE. Direct evidence of surface infestation of seeds and tubers by *Plasmodiophora brassicae* and quantification of spore loads. Plant Pathol. 2011:**60**(5):811–819. https://doi.org/10.1111/j.1365-3059.2011.02449.x

Rolfe SA, Strelkov SE, Links MG, Clarke WE, Robinson SJ, Djavaheri M, Malinowski R, Haddadi P, Kagale S, Parkin IA, et al. The compact genome of the plant pathogen *Plasmodiophora brassicae* is adapted to intracellular interactions with host *Brassica spp*. BMC Genomics. 2016:**17**(1):272. https://doi.org/10.1186/s12864-016-2597-2

Rooney HC, Van't Klooster JW, van der Hoorn RA, Joosten MH, Jones JD, de Wit PJ. Cladosporium Avr2 inhibits tomato Rcr3 protease required for Cf-2-dependent disease resistance. Science. 2005:**308**(5729):1783–1786. https://doi.org/10.1126/science.1111404

Rustgi S, Boex-Fontvieille E, Reinbothe C, von Wettstein D, Reinbothe S. Serpin1 and WSCP differentially regulate the activity of the cysteine protease RD21 during plant development in *Arabidopsis thaliana*. Proc Natl Acad Sci U S A. 2017:**114**(9):2212–2217. https://doi.org/10.1073/pnas.1621496114

Schwelm A, Fogelqvist J, Knaust A, Jülke S, Lilja T, Bonilla-Rosso G, Karlsson M, Shevchenko A, Dhandapani V, Choi SR, et al. The *Plasmodiophora brassicae* genome reveals insights in its life cycle and ancestry of chitin synthases. Sci Rep. 2015:**5**(1):11153. https://doi.org/10.1038/srep11153

Shabab M, Shindo T, Gu C, Kaschani F, Pansuriya T, Chintha R, Harzen A, Colby T, Kamoun S, van der Hoorn RA. Fungal effector protein AVR2 targets diversifying defense-related cys proteases of tomato. Plant Cell. 2008:**20**(4):1169–1183. https://doi.org/10.1105/tpc.107.056325

Shindo T, Kaschani F, Yang F, Kovács J, Tian F, Kourelis J, Hong TN, Colby T, Shabab M, Chawla R, et al. Screen of non-annotated small secreted proteins of *Pseudomonas syringae* reveals a virulence factor that inhibits tomato immune proteases. PLoS Pathog. 2016:**12**(9):e1005874. https://doi.org/10.1371/journal.ppat.1005874

Shindo T, Misas-Villamil JC, Hörger AC, Song J, van der Hoorn RA. A role in immunity for *Arabidopsis* cysteine protease RD21, the ortholog of the tomato immune protease C14. PLoS One. 2012:**7**(1):e29317. https://doi.org/10.1371/journal.pone.0029317

Siemens J, Nagel M, Ludwig-Muller J, Sacristan MD. The interaction of *Plasmodiophora brassicae* and *Arabidopsis thaliana*: parameters for disease quantification and screening of mutant lines. J Phytopathol. 2012:**150**(11–12):592–605. https://doi.org/10.1046/j.1439-0434.2002.00818.x

Smalle J, Vierstra RD. The ubiquitin 26S proteasome proteolytic pathway. Annu Rev Plant Biol. 2004:**55**(1):555–590. https://doi.org/10.1146/annurev.arplant.55.031903.141801

Stegmann M, Anderson RG, Ichimura K, Pecenkova T, Reuter P, Žárský V, McDowell JM, Shirasu K, Trujillo M. The ubiquitin ligase PUB22 targets a subunit of the exocyst complex required for PAMP-triggered responses in *Arabidopsis*. Plant Cell. 2012:**24**(11):4703–4716. https://doi.org/10.1105/tpc.112.104463

Tang L, Yang G, Ma M, Liu X, Li B, Xie J, Fu Y, Chen T, Yu Y, Chen W, et al. An effector of a necrotrophic fungal pathogen targets the calcium-sensing receptor in chloroplasts to inhibit host resistance. Mol Plant Pathol. 2020:**21**(5):686–701. https://doi.org/10.1111/mpp.12922

Toruno TY, Stergiopoulos I, Coaker G. Plant-pathogen effectors: cellular probes interfering with plant defenses in spatial and temporal manners. Annu Rev Phytopathol. 2016:**54**(1):419–441. https://doi.org/10.1146/annurev-phyto-080615-100204

Vlot AC, Dempsey DA, Klessig DF. Salicylic acid, a multifaceted hormone to combat disease. Annu Rev Phytopathol. 2009:**47**(1):177–206. https://doi.org/10.1146/annurev.phyto.050908.135202

Wang S, Xing R, Wang Y, Shu H, Fu S, Huang J, Paulus JK, Schuster M, Saunders DGO, Win J, et al. Cleavage of a pathogen apoplastic protein by plant subtilases activates host immunity. New Phytol. 2021:**229**(6):3424–3439. https://doi.org/10.1111/nph.17120

Yamada K, Matsushima R, Nishimura M, Hara-Nishimura I. A slow maturation of a cysteine protease with a granulin domain in the vacuoles of senescing *Arabidopsis* leaves. Plant Physiol. 2001:**127**(4):1626–1634. https://doi.org/10.1104/pp.010551

Yang G, Tang L, Gong Y, Xie J, Fu Y, Jiang D, Li G, Collinge DB, Chen W, Cheng J. A cerato-platanin protein SsCP1 targets plant PR1 and contributes to virulence of *Sclerotinia sclerotiorum*. New Phytol. 2018:**217**(2):739–755. https://doi.org/10.1111/nph.14842

Yu F, Wang S, Zhang W, Tang J, Wang H, Yu L, Zhang X, Fei Z, Li J. Genome-wide identification of genes encoding putative secreted E3 ubiquitin ligases and functional characterization of PbRING1 in the biotrophic protist *Plasmodiophora brassicae*. Curr Genet. 2019:**65**(6):1355–1365. https://doi.org/10.1007/s00294-019-00989-5

Zhan ZX, Liu HS, Yang Y, Liu S, Li XA, Piao ZY. Identification and characterization of putative effectors from *Plasmodiophora brassicae* that suppress or induce cell death in *Nicotiana benthamiana*. Front Plant Sci. 2022:**13**:881992. https://doi.org/10.3389/fpls.2022.881992

Zhou B, Zeng L. Conventional and unconventional ubiquitination in plant immunity. Mol Plant Pathol. 2017:**18**(9):1313–1330. https://doi.org/10.1111/mpp.12521

Zhou JM, Zhang YL. Plant immunity: danger perception and signaling. Cell. 2020:**181**(5):978–989. https://doi.org/10.1016/j.cell.2020.04.028

Ziemann S, van der Linde K, Lahrmann U, Acar B, Kaschani F, Colby T, Kaiser M, Ding Y, Schmelz E, Huffaker A, et al. An apoplastic peptide activates salicylic acid signalling in maize. Nat Plants. 2018:**4**(3):172–180. https://doi.org/10.1038/s41477-018-0116-y